

CONTROL OF NITRIFICATION EFFICIENCY IN A NEW BIOFILM REACTOR

LAZAROVA V.* , R. NOGUEIRA** , J. MANEM* and L. MELO**

*Centre of International Research for Water and Environment (CIRSEE), Lyonnaise des Eaux,
38, rue du Président Wilson, 78230 Le Pecq, France

** University of Minho, Dept. Bioengineering, 4700 BRAGA, Portugal

ABSTRACT

The study of the nitrification capacity of a new gas-lift circulating bed reactor (CBR) carried out with a laboratory and an industrial scale prototypes, showed a high nitrification rate ($1.2-2 \text{ kgN m}^{-3} \text{ d}^{-1}$) without any nitrite accumulation. A good nitrification performance $0.5-0.6 \text{ kgN m}^{-3} \text{ d}^{-1}$ was maintained even when the $\text{COD}_5/\text{N-NH}_4$ ratio was increased up to 1.8-3.4 (laboratory CBR) and 4-10 (industrial prototype). The comparison of the apparent and intrinsic kinetics indicates that the CBR ensures high specific nitrification rates closed to the maximum value. These results indicate an effective control of the attached biomass growth and activity in this type of bioreactor.

The intrinsic kinetics and diffusion limitations were studied by respirometric essays. It was demonstrated that apparent kinetics are zero-order for bulk concentrations of ammonia above 2 mgN l^{-1} and half-order for lower substrate concentrations. The diffusivity values calculated using the half-order diffusion-reaction model are in the range of 1.09×10^{-9} to $1.58 \times 10^{-9} \text{ m}^2 \text{ s}^{-1}$ for ammonia nitrogen and of 1.1×10^{-9} to $1.37 \times 10^{-9} \text{ m}^2 \text{ s}^{-1}$ for nitrite within the range of temperature studied ($16^\circ-28^\circ\text{C}$). The application of the diffusion-reaction model requires a very precise determination of the biofilm thickness or density. In the case of biofilms developed in heterogeneous granular surfaces, new methods have to be developed for the best estimation of the biofilm density and active cells distribution.

In conclusion it can be stated that this new three-phase bioreactor ensures a high nitrification rate and enhanced process stability through an effective biofilm control. The CBR is a good tool for more fundamental studies of biofilm kinetics and activity thanks to the homogeneous distribution of the fixed biomass in the reactor.

KEY WORDS

nitrification, kinetics, wastewater treatment, new bioreactor, floating media, circulating bed, specific nitrification rate, diffusion-reaction model.

INTRODUCTION

The new European standards for nitrogen and phosphorous removal (EC urban wastewater treatment Directive from 1994) will lead to the upgrading of some of the existing sewage-treatment works and to the conception of new intensive advanced technologies. Biofilm processes are a good alternative for improved nitrogen removal because of their compacity and high nitrification rate. Submerged biological filters have been applied for tertiary nitrification (Pujol *et al.*, 1992). The main disadvantage of these fixed bed reactors is the clogging of the biofilm media. To avoid backwashing problems, a new generation of mobile bed reactors have been developed. The driving force of these processes is the gas injection which ensures important advantages such as high removal efficiency, high nitrification rate, no clogging problems and better mass transfer alongside a simple design and operation. Two types of mobile bed gas-lift reactors have been recently developed on an industrial scale (Heijnen *et al.* 1993 and Hem *et al.*, 1994). The purpose of this paper is to present the nitrification performance of a new gas-lift mobile bed reactor, the circulating bed reactor (CBR) (Lazarova *et al.*, 1995).

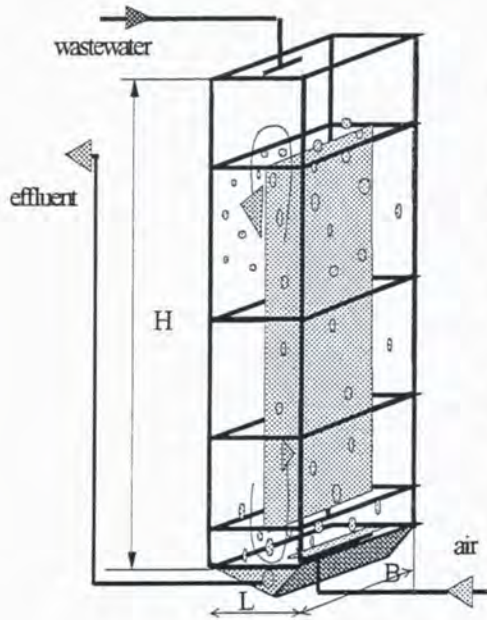


Fig. 1 The circulating bed reactor configuration

Experimental set-up

The circulating bed reactor (CBR) is characterized by (1) the separation of the reactor in two sections: an up-flow aerated section and a down-flow non aerated section, (2) the introduction of a floating media and (3) the induction by the injection of air of a homogeneous three-phase circulation (liquid-gas- solid). The reactor design is simple without any complex technical devices (easier effluent and air-flow distribution, no primary settling, no backwashing).

The geometry and operating conditions of the laboratory scale reactor and industrial-scale prototype are summarized in Table 1. The solid medium used is a rough plastic granular product on the basis of polyethylene with a diameter between 0.5 and 3 mm and a density below and close to the liquid density. The bioreactors are partly filled with these carriers with an average solid hold-up of 15 and 20% for the laboratory and the industrial scale CBR respectively. Both reactors were seeded in batch with activated sludge according to a specific start-up procedure (Lazarova *et al.*, 1994) therefore ensuring a good equilibrium between *Nitrosomonas* and *Nitrobacter* populations.

Table 1 Geometry and operating conditions of the circulating bed reactors

Parameters	Laboratory scale reactor	Industrial scale prototype	
		secondary nitrification	tertiary nitrification
Liquid volume, m ³	0.0046		4.6
Length, L=B, m	0.09		0.9
Height, H, m	0.6		6
Gas velocity, m s ⁻¹	0.012- 0.035	0.01-0.02	0.02-0.027
Feed flow rate, m ³ h ⁻¹	0.0048	from 1.15 to 3	from 2 to 8
Hydraulic residence time, HRT, h	1	from 4 to 1,5	from 2.3 to 0,5
Loading rate, kgN m ⁻³ d ⁻¹	1-1.2	0.15-0.7	0.5-2.5

Wastewater characteristics and analytical methods

The biological performance of the new bioreactor is investigated in an industrial-scale prototype for secondary and tertiary nitrification of municipal wastewater (Table 2). Synthetic medium with the similar ammonia and COD content was used in the laboratory scale experiments.

Table 2 Average influent wastewater characteristics in the industrial scale prototype

Parameters	Influent after primary settling tank	Influent after secondary treatment
Temperature, °C	12-17	16- 22
pH	7.1-7.3	6.2-7.5
Ammonia nitrogen, gN m ⁻³	50 (25-70)*	50 (20-68)
Dissolved COD, g m ⁻³	180 (120-320)	53 (32-175)
Dissolved BOD ₅ , g m ⁻³	55 (35-125)	8 (3-10)
Orthophosphates, g m ⁻³	9 (8-11)	8 (6-9.5)
Suspended solids, g m ⁻³	120 (100-250)	9 (6-120)
Alkalinity, gCaCO ₃ m ⁻³	350 (320-450)	210 (168-238)

*average value (minimal - maximal value) from 6-24 h mixed samples

All forms of nitrogen are measured immediately after sampling and filtration (0,45µ) by the colorimetric methods Hach and calibrated weekly with the values obtained with a Technicon Instrumentals apparatus. The soluble carbon pollution is evaluated by the chemical oxygen demand after filtration, CODs, according to the micro-technique of the *Standard Methods*. The experiments for tertiary nitrification in the industrial-scale CBR were performed adjusting the ammonia nitrogen and alkalinity in the secondary treated effluent by means of two synthetic solutions of ammonia sulfate and sodium carbonate. All results are expressed on the basis of total bioreactor volume.

Biofilm activity characterization

The biofilm composition was estimated by means of protein, polysaccharides, COD and dry weight measurements described in more detail elsewhere (Lazarova *et al.*, 1994a). Total protein (PR) was chosen as the basic descriptor of the active biomass. The bioreactor performance was evaluated by the apparent volumetric (r_N , gN m⁻³ d⁻¹) and specific (k_N , gN-NH₄ g⁻¹ PR d⁻¹) nitrification rate:

$$r_N = \frac{S_0 - S}{\theta} \quad (1)$$

$$k_N = \frac{S_0 - S}{X\theta} \quad (2)$$

where S_0 and S are the initial and effluent substrate concentration (mg l^{-1}); X is the fixed biomass concentration expressed by the protein content in the total reactor volume (g l^{-1}), θ is hydraulic retention time, (HRT h), calculated on the basis of the overall reactor volume.

Kinetics and diffusion limitation studies

Biological Oxygen Monitor (MYSI 15) was used for the measurement of biofilm specific activity r_{O_2} , $\text{gO}_2 \text{ g}^{-1} \text{ PR d}^{-1}$ (Walker and Davis, 1977). Intrinsic kinetic constants of the biofilm were derived therefrom. The respirometry test device has a volume of 10 ml, is well closed with a tightly fitting stopper and the suspension is mixed with a magnetic stirrer to overcome external mass transfer resistance. Oxygen depletion is monitored continuously by a YSI electrode and the temperature was controlled by water bath. The batch respirometric experiments were performed as follows: 10 ml of phosphate buffer were saturated with oxygen by air bubbling and stirring during 30 min, 1 ml of plastic beads were put on, the respirometric cell was closed and endogenous oxygen consumption was monitored. Then, an exogenous substrate (ammonium, nitrite or acetate) was added by syringe through the stopper and the maximum specific activity was calculated from the oxygen consumption curve.

Supplementary kinetic experiments were performed in the respirometer with the biofilm from the laboratory-scale CBR to study the influence of ammonia and nitrite nitrogen concentration on reaction rates for different temperatures. Kinetics constants were calculated according to the diffusion-reaction model in porous catalysts described by Harremoës (1978). External diffusion was not considered to be limiting due to the intense mixing of the three-phase flow. The overall reaction rate involved the interaction between internal diffusion of nutrients and biochemical reactions in the biofilm. In the reaction limited case:

$$r_a = k_{oa} \quad (3)$$

$$k_{oa} = k_{of} * L_f \quad (4)$$

In the diffusion limited case:

$$r_a = k_{1/2a} * S^{1/2} \quad (5)$$

$$k_{1/2a} = \sqrt{2D_f k_{of}} \quad (6)$$

The diffusion coefficient was calculated from the following equation (eq. 7) which is a rearrangement of eq. 6:

$$D_f = \frac{k_{1/2a}^2}{2k_{of}} * L_f \quad (7)$$

where k_{oa} ($\text{g m}^{-2} \text{ d}^{-1}$) and $k_{1/2a}$ ($\text{g}^{1/2} \text{ m}^{-1/2} \text{ d}^{-1}$) are zero order and half order rate constants per unit of biofilm surface; k_{of} ($\text{g m}^{-3} \text{ d}^{-1}$) zero order rate constant per unit biofilm volume; L_f (m) biofilm thickness and D_f ($\text{m}^2 \text{ s}^{-1}$) biofilm effective diffusivity.

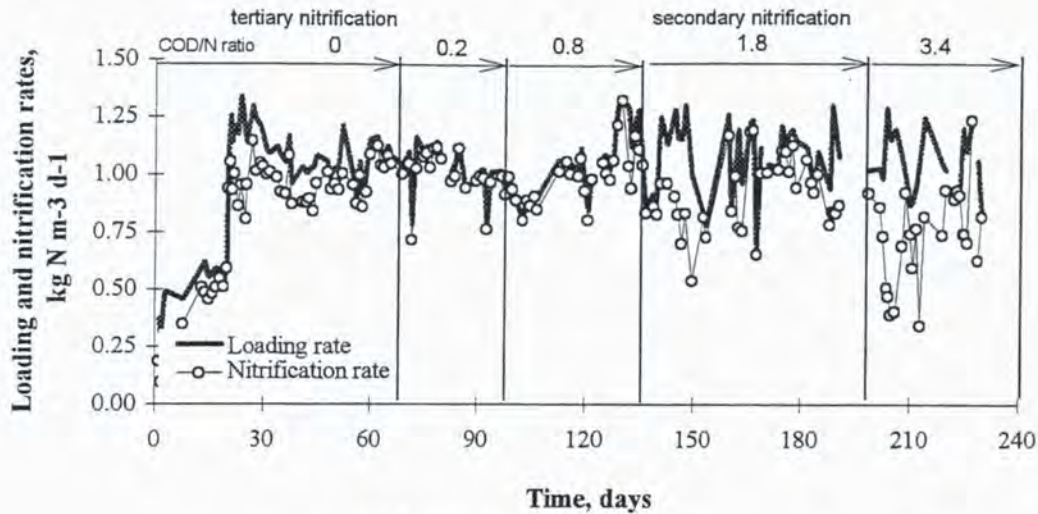
RESULTS AND DISCUSSION

Nitrification capacity of the CBR

Figure 2a compares the evolution of the nitrification rate r_N (eq. 1) at laboratory scale CBR as a function of time and operating conditions (COD_5/N ratio). After a short two weeks' period of start-up, the nitrification rate increases from 0.3-0.5 to 1-1.2 $\text{kgN m}^{-3} \text{ d}^{-1}$. This good nitrification activity is maintained under conditions of stepwise increase of the COD_5/N ratio up to 1.8. Furthermore, nitrification effectiveness decreases from 90-95% to 60-70% ($r_N=0.5-0.7 \text{ kgN m}^{-3} \text{ d}^{-1}$). In all conditions, total removal of organic carbon is observed.

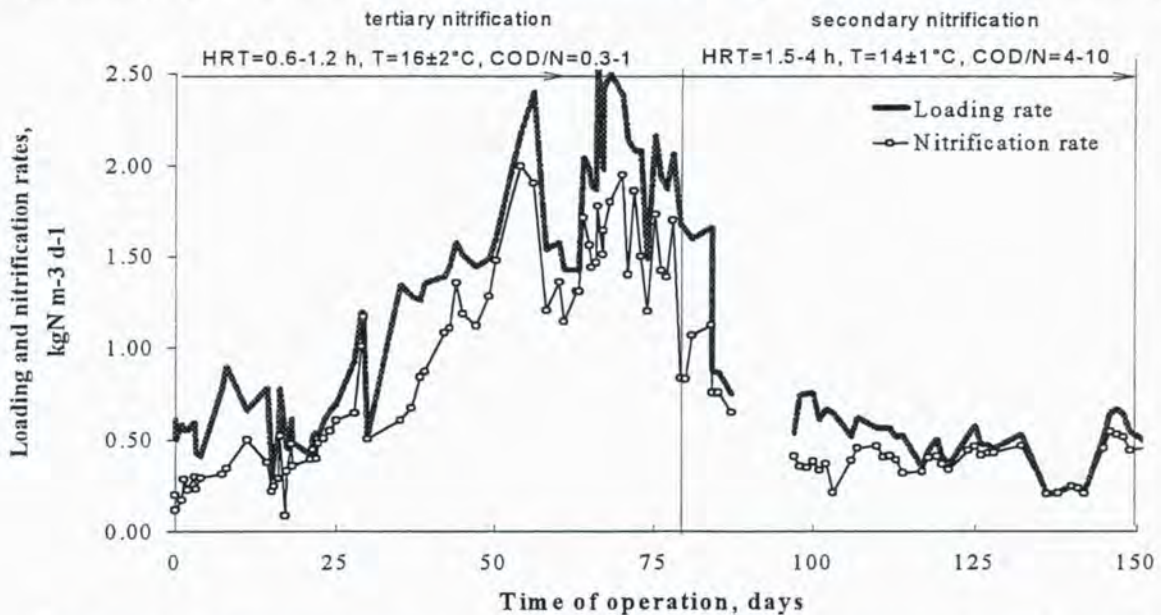
Despite to the lower temperature ($16 \pm 2^\circ\text{C}$ compared with $25 \pm 2^\circ\text{C}$ in lab-scale reactor), the start-up period of the industrial scale CBR is also relatively brief: two weeks to reach $0.5 \text{ kgN m}^{-3} \text{ d}^{-1}$ and 2 months to attain a maximum nitrification rate r_N of $2 \text{ kgN m}^{-3} \text{ d}^{-1}$ (Fig. 2b). After the change of the influent from secondary to primary settled sewage, the nitrification rate dropped sharply and stabilized rapidly at $0.5-0.6 \text{ kgN m}^{-3} \text{ d}^{-1}$. Total carbon elimination is observed

with removal rate r_{COD} up to $5 \text{ kg COD}_s \text{ m}^{-3} \text{ d}^{-1}$. The mean value of the effluent CODs concentration is about 50 mg l^{-1} ($\text{BOD}_5 < 5 \text{ mg l}^{-1}$) and is not modified for all loading tested. These results demonstrate that nitrification is the limiting step in combined carbon and nitrogen removal.



a) laboratory scale experiments

(HRT=1 h, $S_{\text{o},\text{N-NH}_4}=50\pm 10 \text{ mg l}^{-1}$, oxygen concentration $6\pm 2 \text{ mg l}^{-1}$, $S_{\text{N-NO}_2}<1.5 \text{ mg l}^{-1}$, $T=25\pm 2^\circ\text{C}$)



b) industrial scale experiments ($S_{\text{o},\text{N-NH}_4}=40\pm 10 \text{ mg l}^{-1}$, $S_{\text{o},\text{COD}_s}=230\pm 60 \text{ mg l}^{-1}$, $S_{\text{N-NO}_2}<1.0 \text{ mg l}^{-1}$)

Fig. 2 Evolution of nitrification rate in the laboratory (a) and at industrial scale CBR (b)

Table 3 Comparison between apparent nitrification kinetics (eq. 2) and the intrinsic values calculated from the respirometry tests (eq. 8)

	Nitrification kinetics, $\text{gN g}^{-1} \text{ PR d}^{-1}$	
	Apparent measured values k_{N}	Intrinsic values $k_{\text{N,int}}$ (respirometry tests)
Laboratory scale CBR		
tertiary nitrification	2.58 ± 1.26 (1.2-5.2)*	2.9
secondary nitrification	0.92 ± 0.26 (0.53-1.2)	1.39 ± 0.18 (1.22-1.65)
Industrial prototype		
tertiary nitrification	1.88 ± 0.26 (1.4-2.3)	0.99 ± 0.17 (0.8-1.25)
secondary nitrification	0.22 ± 0.07 (0.1-0.3)	0.3 ± 0.03 (0.26-0.32)

*average value \pm standard deviation (minimum-maximum value)

Biofilm kinetics

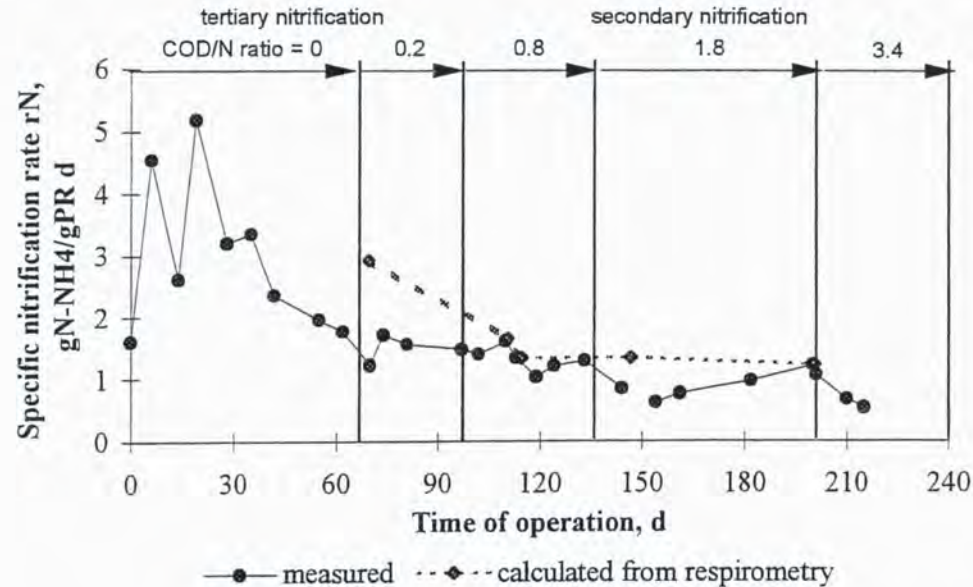
Apparent nitrification kinetics k_{N} at both laboratory and industrial scale CBR are calculated using equation (2) and compared with intrinsic parameters $k_{\text{N,int}}$ measured by respirometric tests (Fig. 3a and Fig. 3b):

$$k_{\text{N,int}} = \frac{r_{\text{O}_2}}{4.57} \quad (8)$$

where 4.57 is the yield coefficient for oxygen consumption during ammonia oxidation and r_{O_2} is the maximum specific respiration activity of the CBR biofilm ($\text{gO}_2 \text{ g}^{-1} \text{ PR d}^{-1}$).

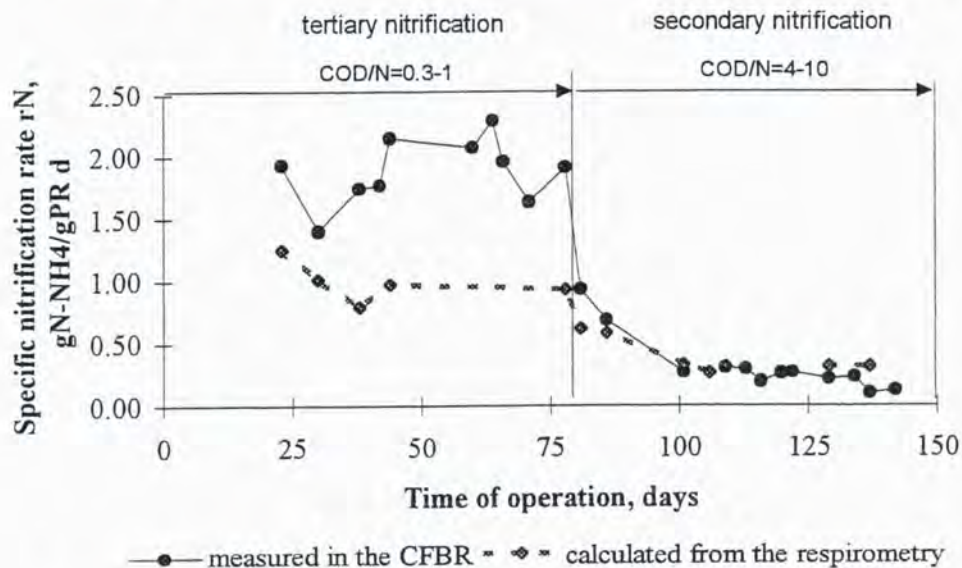
Specific nitrification rate is strongly influenced by the increasing COD/N ratio. This trend is more pronounced in the industrial prototype where the mean specific nitrification rate decreases from 1.88 to 0.22 gN g⁻¹ PR d⁻¹ immediately after the change of the secondary treated influent by primary settled sewage (Fig. 3b and Table 3). The intrinsic values calculated from the maximum respiration activity correlate well with the observed apparent kinetics in the case of secondary nitrification (Fig. 3 and Table 3). However, discrepancies are observed for the values measured during the tertiary nitrification at industrial scale prototype where the calculated intrinsic values (0.99 gN g⁻¹ PR d⁻¹) are lower than apparent kinetics (1.88 gN g⁻¹ PR d⁻¹). This fact could be explained by the better oxygen transfer in the three phase flow of the CBR compared with the stirred oxygen monitor.

It is important to notice that in conditions of tertiary nitrification the specific apparent and intrinsic nitrification rates are rather similar at both laboratory and industrial scale CBR (2.58±1.26 compared to 1.88±0.26 gN g⁻¹ PR d⁻¹).



a) laboratory scale experiments

(HRT=1 h, $S_{o,N-NH_4}=50\pm 10$ mg l⁻¹, oxygen concentration 6 ± 2 mg l⁻¹, $T=25\pm 2^\circ C$)



b) industrial scale experiments ($S_{o,N-NH_4}=40\pm 10$ mg l⁻¹, $S_{o,COD_s}=230\pm 60$ mg l⁻¹)

Fig. 3 Comparison of the specific nitrification rate measured in the CBR and the intrinsic rate calculated from respirometric tests

Application of diffusion-reaction model on kinetics study of the CBR biofilm

For a better understanding of the CBR nitrification performance, complementary respirometric kinetics experiments are performed with the thicker biofilm from the laboratory scale CBR to study the influence of ammonia and nitrite nitrogen concentration on reaction rate. To obtain the zero order intrinsic kinetic constant of the biofilm, k_{of} , it is necessary to measure the biofilm thickness. In this study the biofilm thickness was determined approximately, based on the biofilm

density, the specific surface area of the carrier and the dry weight of the biofilm. Because of the inhomogenous biomass distribution a supplementary hypothesis must be put forward for the percentage of the colonized surface area. Two extreme values are utilized: total 100% surface coverage by the biofilm ($L_f=122 \mu$) and 50% colonized surface ($L_f=244 \mu$) which corresponds better on visual observations of the inhomogenous biofilm distribution.

The relationship between the overall nitrification rate (r_a , eq.3) and nitrogen concentration for the first case studied ($L_f=122 \mu$) is shown in Figure 4. A linear dependency of the reaction rate on substrate concentration (ammonia or nitrite nitrogen) is found, until the reaction rate reaches a constant value. The transition concentration of ammonia and nitrite nitrogen from a diffusion limited case to a reaction limited case is calculated from eq. 3 and 5 (Table 4). The overall reaction rate is considered to be limited by the biochemical reaction in case of a $[O_2/N-NH_4]$ or $[O_2/N-NO_2]$ ratios less than the transition values listed in Table 4.

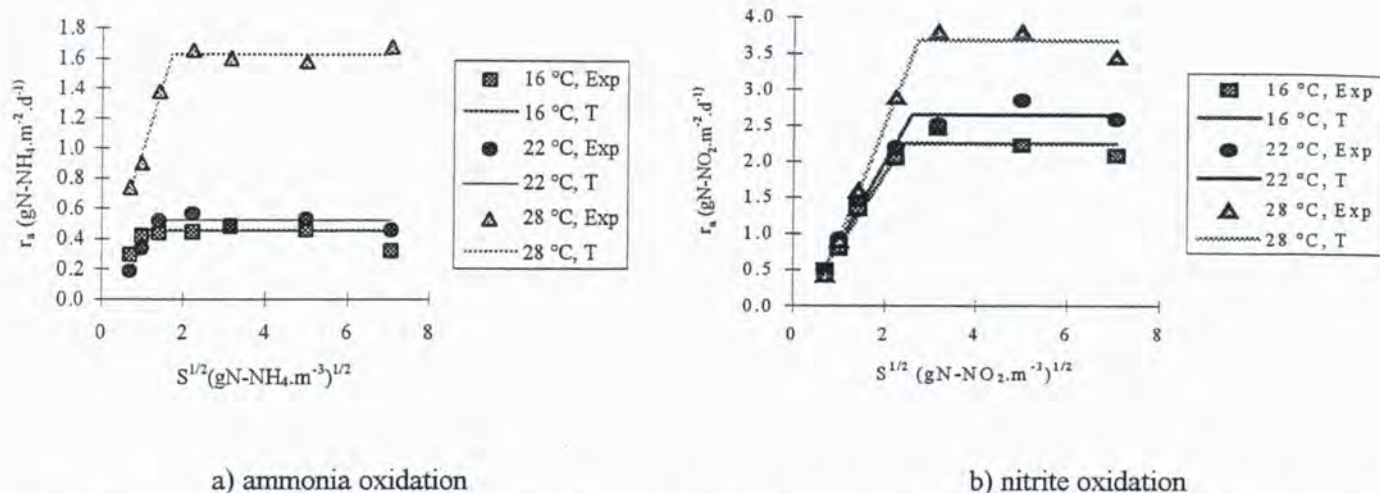


Fig. 4 Dependence of nitrification rate on bulk ammonia (a) and nitrite (b) concentration for different temperature (biofilm thickness 122 μ)

Table 4. Characteristic values for transition from half order apparent reaction rate to zero order reaction rate

T (°C)	O ₂ solubility (mg l ⁻¹)	N-NH ₄ (mg l ⁻¹)	O ₂ /N-NH ₄ (-)	N-NO ₂ (mg l ⁻¹)	O ₂ /N-NO ₂ (-)
16	9.9	1.1	8.7	5.6	1.8
22	8.4	2.0	4.2	6.7	1.3
28	7.8	3.0	2.7	7.4	1.1

occurred at about 2.7 and 3.2 gO₂/gN-NH₄, at an oxygen concentration of 9-10 and 6 mgO₂ l⁻¹ respectively.

The zero order rate constants, k_{oa} for the reaction limited conditions (eq. 3, Table 5) are calculated as the mean values for ammonia or nitrite nitrogen concentrations greater then the respective transition values. For the diffusion limited conditions, the overall reaction rate r_a is a function of the root of the bulk nitrogen concentration (eq. 5). The slope of the curves (Fig. 4) corresponds to the half order rate constant $k_{1/2a}$.

Table 5 Kinetic constants in the CBR calculated for two different biofilm thickness

Substrate	T (°C)	100% of the surface area is covered by the biofilm, $L_f=122 \mu$						50% of the surface area is covered, $L_f=244 \mu$				
		k_{oa} (g m ⁻² d ⁻¹)	k_{of} (g m ⁻³ d ⁻¹)	$k_{1/2a}$ (g ^{1/2} m ^{-1/2} d ⁻¹)	D_f (m ² s ⁻¹)	$D_f/D_w^{a)}$	$D_f/D_w^{b)}$	k_{oa} (g m ⁻² d ⁻¹)	k_{of} (g m ⁻³ d ⁻¹)	$k_{1/2a}$ (g ^{1/2} m ^{-1/2} d ⁻¹)	D_f (m ² s ⁻¹)	$D_f/D_w^{b)}$
N-NH ₄	16	0.45	3.66E+03	0.42	2.8E-10	0.18	0.25	0.91	3.66E+03	0.84	1.1E-09	0.96
	22	0.52	4.29E+03	0.45	2.9E-10	0.16	0.21	1.02	4.29E+03	1.0	1.4E-09	0.99
	28	1.63	1.34E+04	0.92	3.7E-10	0.17	0.22	3.26	1.34E+04	1.9	1.6E-09	0.95
N-NO ₂	16	2.20	1.80E+04	1.01	3.3E-10	0.22	0.28	4.5	1.80E+04	1.87	1.2E-09	0.95
	22	2.65	2.17E+04	1.12	3.3E-10	0.19	0.23	5.3	2.17E+04	2.05	1.4E-09	0.79
	28	3.69	3.02E+04	1.61	5.0E-10	0.24	0.29	7.37	3.02E+04	2.68	1.7E-09	0.81

Note: D_{w,NO_2} in water was assumed to be equal to the D_{w,NO_3} ;

a) D_{w,NO_2} and D_{w,NO_3} were calculated using the Nernst equation;

b) D_{w,NO_2} and D_{w,NO_3} were calculated using the Nernst-Haskell equation for the counterion SO_4^{2-} and Na^+ , respectively.

The diffusivity values calculated using the half-order diffusion reaction model and a biofilm thickness of 122 μ are in the range of 2.83×10^{-10} to $3.68 \times 10^{-10} \text{ m}^2 \text{ s}^{-1}$ for ammonium and of 3.3×10^{-10} to $4.96 \times 10^{-10} \text{ m}^2 \text{ s}^{-1}$ for nitrite within the range of temperature studied (from 16° to 28°C). Compared with the diffusivity in water, these values are too low, about 20%. The calculated zero and half order rate constants k_{oa} and $k_{1/2a}$ for the ammonia nitrogen are in the range of 0.45-1.63 $\text{g m}^{-2} \text{ d}^{-1}$ and 0.42-92 $\text{g}^{1/2} \text{ m}^{-1/2} \text{ d}^{-1}$ and for nitrite nitrogen in the range of 2.2-3.69 $\text{g m}^{-2} \text{ d}^{-1}$ and 1.01-1.61 $\text{g}^{1/2} \text{ m}^{-1/2} \text{ d}^{-1}$ respectively. The comparison of these results with the values obtained with the assumption of 50% surface coverage ($L_f=244 \mu$) shows the great importance of the correct measurement of the biofilm thickness. Thus, for the thicker biofilm the calculated zero and half order rate constants k_{oa} and $k_{1/2a}$ are two times higher than those obtained in the case of 100% surface coverage. The calculated diffusion coefficient of NH_4^+ and NO_2^- also varied from 23-27% to 79-100% of the respective values in water for 100% and 50% colonized surface respectively.

The experimental studies of diffusion coefficients for NH_4^+ and NO_2^- through nitrifying biofilms found in literature are very limited (Table 6). Williamson and McCarty (1976) and Onuma and Omura (1982) used the diffusion cell method which consists of dispersing acclimated activated flocs onto a porous filter. The ammonia diffusion coefficient in these artificial biofilms are respectively 87 and 76% of their corresponding values in water.

Table 6 Experimental values of NH_4^+ and NO_2^- diffusion coefficients within biofilms

Authors	Substrate	$D_f \times 10^{-9}$ ($\text{m}^2 \text{ s}^{-1}$)	D_f/D_w^*	Biofilm type	Growth system	Experimental method
Williamson and McCarty (1976)	NH_4^+	1.50	0.87	Nitrifying culture floc	Downflow column packed with plastic beads	Diffusion cell (20°C, pH=7)
	NO_2^-	1.39	0.86			
Harremoës (1981)	$\text{NH}_3\text{-N}$	1.95	-	-	-	Diffusion reaction model
Onuma and Omura (1982)	NH_4^+	1.28	0.76	Nitrifying culture floc	Activated sludge	Diffusion cell (20°C, pH=7.8)
This study ($L_f=244 \mu$)	NH_4^+	1.38	0.99	CBR plastic granules		Diffusion reaction model (22°C, pH=7.8)
	NO_2^-	1.12	0.79			

* the NH_4^+ and NO_2^- aqueous diffusion coefficients (D_w) were calculated using the Nernst equation

According to literature data (Table 7), the values of the apparent kinetic constants depend on the biofilm reactor type, biofilm composition and on the operating conditions, especially on the dissolved oxygen concentration. Toettrup *et al.* (1994), Hem *et al.* (1994) and Çeçen (1995) reported values that are in the range of the values obtained in the present study.

Table 7 Kinetic parameters of different nitrifying biofilms

Author	Substrate	k_{oa} ($\text{g m}^{-2} \text{ d}^{-1}$)	k_{of} ($\text{g m}^{-3} \text{ d}^{-1}$)	$k_{1/2a}$ ($\text{g}^{1/2} \text{ m}^{-1/2} \text{ d}^{-1}$)	Biofilm Reactor
Harremoës (1981)	$\text{NH}_4\text{-N}$	9.6	6×10^4	4.5	Rotating Drum ($L=160 \mu\text{m}$, $\text{DO}>22 \text{mg/l}$)
Onuma and Omura (1982)	$\text{NH}_4\text{-N}$	21.6	1.74×10^5	5.578	Circulating Filter (20°C, pH=7.8) (20°C, pH=7.7)
	$\text{NO}_2\text{-N}$	19.92	1.53×10^5	5.138	
Toettrup <i>et al.</i> (1994)	$\text{NH}_4\text{-N}$	1.7		1.26	Floating Filter (DO>7mg/l) Tertiary Nitrification Lab-Scale Tertiary Nitrification Full-Scale
		1.35			
Hem <i>et al.</i> (1994)	$\text{NH}_4\text{-N}$	0.7-1	-	-	Moving Bed Biofilm Reactor (DO=4.5-5mg/l)
Çeçen (1995)	$\text{NH}_4\text{-N}$	1.82	-	0.9	Submerged Nitrification Filter (DO=4.5mg/l) (DO=2.3mg/l)
		0.47			
This study ($L_f=244 \mu$)	$\text{NH}_4\text{-N}$	1.02	4.16×10^4	1.0	Circulating Bed Reactor plastic granules (22°C, pH=7.8)
	$\text{NO}_2\text{-N}$	5.3	2.17×10^4	2.05	

The kinetics parameters of the CBR biofilm were estimated with the assumption of an average biofilm density of 35 kg m^{-3} . However, this value is not representative for the real concentration of active bacteria, in particular of nitrifiers. According to the results on population dynamics obtained by RNA probe analysis (Lazarova *et al.*, 1995) only 13.3% of the biofilm mass in the biofilm from the tertiary nitrification studies is ammonia oxidizers. Thus, the real concentration or density of nitrifying population would be 4.65 kg m^{-3} . This value is used to compare the calculated zero order rate constant of the CBR biofilm k_{of} (from Table 5) with the values estimated by Nogueira (1996) on the basis of kinetics of an enriched nitrifying suspended culture (Table 8):

$$k_{of} = k_x \cdot X_a \quad (9)$$

where k_x ($\text{gN g}^{-1} \text{ SS d}^{-1}$) is the maximum nitrification rate of the suspended nitrifying culture and X_a (kg m^{-3}) the concentration of active bacteria in the biomass.

Table 8 Comparison between the zero order kinetics k_{of} obtained by the diffusion-reaction model and those estimated from the maximum nitrification rate in suspended culture

T°C	Biofilm k_{of} $\text{gN m}^{-3} \text{ d}^{-1}$	Kinetics estimation from suspended culture		
		k_x $\text{gN g}^{-1} \text{ SS d}^{-1}$	Biomass density, kg m^{-3}	
			35	4.65
16	3.66×10^3	0.74	$2.58 \cdot 10^4$	$3.56 \cdot 10^3$
22	4.29×10^3	0.94	$3.28 \cdot 10^4$	$4.54 \cdot 10^3$
28	1.34×10^4	1.02	$3.57 \cdot 10^4$	$4.94 \cdot 10^3$

From the results presented in Table 8 it can be seen that the density of 35 kg m^{-3} is a value too high to represent the real density of active bacteria in the CBR biofilm. A better fitting between the results obtained by the diffusion-reaction model and those calculated on the basis of the maximum nitrification rate of suspended nitrification culture is done by a hypothetical density approximated by dynamic population estimation. Furthermore, new methods such as

the RNA probe analysis must be used for a more accurate active cell density determination in inhomogenous biofilms.

CONCLUSIONS

The results of the study of a new gas-lift reactor, the circulating bed CBR, obtained with laboratory and industrial scale prototypes could be summarized as follows:

- (1) The CBR shows high nitrification rates under condition of tertiary nitrification ranging from 1.2 to $2 \text{ kgN m}^{-3} \text{ d}^{-1}$ without any nitrite accumulation. A good nitrification performance 0.5 - $0.6 \text{ kgN m}^{-3} \text{ d}^{-1}$ was maintained also in secondary nitrification.
- (2) The specific nitrification activity for the tertiary nitrification remained quasi constant in both laboratory and industrial scale reactors, i.e. 2.3 and $1.8 \text{ kgN-NH}_4 \text{ kg}^{-1} \text{ protein d}^{-1}$. The high COD/N ratio up to 10 in the secondary treatment induced a strong reduction in the specific nitrification rate down to $0.22 \text{ kgN-NH}_4 \text{ kg}^{-1} \text{ protein d}^{-1}$.
- (3) The intrinsic kinetic values calculated from the maximum respiration activity correlate well with the observed apparent kinetics in secondary nitrification. These results indicate an effective control of the attached biomass growth and activity.
- (4) The respirometric essays with the thicker biofilm from the laboratory CBR demonstrated that apparent kinetics are zero-order for substrate concentration above 2 mgN dm^{-3} and half-order respectively for 0.5 - 2 mgN dm^{-3} . The diffusivity values calculated using the half-order diffusion-reaction model and assuming that 50% of the solid surface is colonized were in the range of 1.09×10^{-9} to $1.58 \times 10^{-9} \text{ m}^2 \text{ s}^{-1}$ for ammonium and of 1.1×10^{-9} to $1.37 \times 10^{-9} \text{ m}^2 \text{ s}^{-1}$ for nitrite within the range of temperature studied (from 16° to 28°C).

It is important to notice that the application of the diffusion-reaction model requires a very precise determination of the biofilm thickness or density. In the case of biofilms developed in heterogeneous granular surfaces, new methods have to be developed for the best estimation of the biofilm density and active cells distribution.

NOMENCLATURE

B - reactor length (m)

D_f - biofilm effective diffusivity or diffusion coefficient ($\text{m}^2 \text{ s}^{-1}$)

D_w - diffusion coefficient in water ($\text{m}^2 \text{ s}^{-1}$)

H - reactor height, m

k_N - apparent specific nitrification rate ($\text{gN g}^{-1} \text{ protein d}^{-1}$)

$k_{N,int}$ - intrinsic nitrification rate calculated from respirometric tests ($\text{gN g}^{-1} \text{ protein d}^{-1}$)

k_{0a} - zero order rate constant per unit biofilm surface ($\text{g m}^{-2} \text{d}^{-1}$)
 $k_{1/2a}$ - half order rate constants per unit biofilm surface ($\text{g}^{1/2} \text{m}^{-1/2} \text{d}^{-1}$)
 k_{0f} - zero order rate constant per unit biofilm volume ($\text{g m}^{-3} \text{d}^{-1}$)
 k_x - maximum nitrification rate of the suspended nitrifying culture ($\text{gN g}^{-1} \text{SS d}^{-1}$)
 L - reactor width (m)
 L_f = biofilm thickness (m)
 r_a - overall reaction rate ($\text{g.m}^{-2}.\text{d}^{-1}$)
 r_N - apparent volumetric nitrification rate ($\text{gN m}^{-3} \text{d}^{-1}$)
 r_{O_2} - biofilm maximum respiration rate ($\text{gO}_2 \text{g}^{-1} \text{protein d}^{-1}$)
 S - effluent substrate concentration (g.m^{-3})
 S_0 - initial substrate concentration (g.m^{-3})
 X - fixed biomass concentration (g protein l^{-1})
 X_a - concentration of active bacteria in the suspended biomass (kg m^{-3})
 θ - hydraulic retention time (HRT, h)

REFERENCES

- Çeçen F. (1995) Factor for Substrate Removal in Nitrifying and Denitrifying Biofilm Reactors. Proceedings of the International IAWQ Conference Workshop. Biofilm Structure, Growth and Dynamica. Need for New Concepts?. Noordweijkerhout, The Netherlands.
- Gönenç E. and Harremoës P. (1985) Nitrification in Rotating Disc Systems-I, Criteria for Transition From Oxygen to Ammonia Rate Limitation, Water Res. Vol. 19, No. 9, pp. 1119-1127.
- Hem L. J., Rusten B. and Ødegaard H. (1994) Nitrification in a Moving Bed Biofilm Reactor, Wat. Res. Vol. 28, No. 6, pp. 1425-1433.
- Harremoës P. (1978) Biofilm Kinetics. In: Mitchel, R. (ed.) Water Pollution Control Microbiology, Vol. 2, p. 82-109. Jonh Wiley and Sons, New York.
- Harremoës P., Sekoulov I. and Bonomo L. (1981) Design of Fixed Film Nitrification and denitrification Units Based on Laboratory and Pilot Scale Results. Europäische Abwasswe Symposium, Abwassertechnische, München.
- Heijnen J.J., van Loosdrecht, M.C.M., Mulder R., Weltevrede R. and Mulder A. (1993) Development and scale-up of an aerobic biofilm air-lift suspension reactor. *Wat.Sci.Tech.*, 27, No 5-6, 253-261.
- Lazarova V., V. Pierzo D. Fontvieille et J. Manem (1994) Estimation de l'activité des biofilms par la mesure des protéines totales: une nouvelle approche méthodologique. *Colloque "Journées Information Eaux, 28-30 septembre 1994, Poitiers, vol.1, 33/1-33/17.*
- Lazarova V., Pierzo V., Fontvieille D. and Manem J. (1994a) Integrated approach for biofilm characterization and biomass activity control. *Wat. Sci. Tech.* 29, (7), 345-354.
- Lazarova V. and Manem J. (1995) An innovative process for waste water treatment: the circulating floating bed reactor. *18th Biennial Conf. and Exhib.of Wat. Qual. Int.* 96, 23-28 June, Singapore, accepted for oral presentation.
- Nogueira R. (1996) Nitrification kinetic constants of a mixed suspended culture and a biofilm. Thesis, University of Minho.
- Onuma M. and Omura T. (1982) Mass-Transfer Characteristics within Microbiol Systems, *Wat. Sci. Tech.* Vol. 14, pp. 553-568.
- Pujol R., Canler J.P. and Iwema A. (1992) Biological aerated filters: an attractive and alternative biological process. *Wat.Sci.Tech.*, 26, (3-4), 693-702.
- Toettrup H., Rogalla. F., Vidal. A., Harremoës. P., The tratment Trology of Floating Filters: From Pilot to Prototype to Plant, *Wat. Sci. Tech.* Vol. 29, No.10-11, pp. 23-32, 1994.
- Williamson K. and McCarty. P. L. (1976) A model of substrate utilization by bacterial films, *Journal WPCF* Vol. 48, No. 1, pp. 9 - 24.
- Williamson K. and McCarty P. L. (1976) Verification studies of the biofilm model for bacterial substrate utilization, *Journal WPCF* Vol. 48, No. 2, pp. 281 - 296.